Mapping the effects of ozone pollution and mixing on floral odour plumes and their impact on plant-pollinator interactions

Langford, Ben, Ryalls, James W. M. ORCID logoORCID: https://orcid.org/0000-0003-2015-3605, Mullinger, Neil J., Hayden, Paul, Nemitz, Eiko, Pfrang, Christian, Robins, Alan, Touhami, Dalila, Bromfield, Lisa M. and Girling, Robbie D. ORCID logoORCID: https://orcid.org/0000-0001-8816-8075 (2023) Mapping the effects of ozone pollution and mixing on floral odour plumes and their impact on plant-pollinator interactions. Environmental Pollution. 122336. ISSN 0269-7491 doi: https://doi.org/10.1016/j.envpol.2023.122336 (In Press) Available at https://centaur.reading.ac.uk/112993/

It is advisable to refer to the publisher's version if you intend to cite from the work. See Guidance on citing.

To link to this article DOI: http://dx.doi.org/10.1016/j.envpol.2023.122336

Publisher: Elsevier

CentAUR

Central Archive at the University of Reading

Reading's research outputs online

Journal Pre-proof

Mapping the effects of ozone pollution and mixing on floral odour plumes and their impact on plant-pollinator interactions

Ben Langford, James M.W. Ryalls, Neil J. Mullinger, Paul Hayden, Eiko Nemitz, Christian Pfrang, Alan Robins, Dalila Touhami, Lisa M. Bromfield, Robbie D. Girling

Please cite this article as: Langford, B., Ryalls, J.M.W., Mullinger, N.J., Hayden, P., Nemitz, E., Pfrang, C., Robins, A., Touhami, D., Bromfield, L.M., Girling, R.D., Mapping the effects of ozone pollution and mixing on floral odour plumes and their impact on plant-pollinator interactions, *Environmental Pollution* (2023), doi: https://doi.org/10.1016/j.envpol.2023.122336.

This is a PDF file of an article that has undergone enhancements after acceptance, such as the addition of a cover page and metadata, and formatting for readability, but it is not yet the definitive version of record. This version will undergo additional copyediting, typesetting and review before it is published in its final form, but we are providing this version to give early visibility of the article. Please note that, during the production process, errors may be discovered which could affect the content, and all legal disclaimers that apply to the journal pertain.

1 **Mapping the effects of ozone pollution and mixing on floral odour**
2 **plumes and their impact on plant-pollinator interactions**

3 Ben Langford[a*], James M.W. Ryalls[b], Neil J. Mullinger[a], Paul. Hayden[c], Eiko Nemitz[a],
4 Christian Pfrang[d,e,f], Alan Robins[c], Dalila Touhami[d], Lisa M. Bromfield and Robbie D.
5 Girling[b,g]

6 [a]UK Centre for Ecology & Hydrology, Penicuik, Midlothian, EH26 0QB, UK
7 [b]School of Agriculture, Policy and Development, University of Reading, RG6 6EU, UK
8 [c]EnFlo, Department of Mechanical Engineering Sciences, University of Surrey, Guildford, GU2
9 7XH, UK
10 [d]Department of Chemistry, University of Reading, P.O. Box 224, RG6 6AD, Reading, UK
11 [e]School of Geography, Earth and Environmental Sciences, University of Birmingham, B15 2TT, UK
12 [f] Department of Meteorology, University of Reading, P.O. Box 243, RG6 6BB, Reading, UK
13 [g]Centre for Sustainable Agricultural Systems, Institute for Life Sciences and the Environment,
14 University of Southern Queensland, Toowoomba, Queensland 4350, Australia
15
16 *Correspondence: benngf@ceh.ac.uk
17
18 **Highlights:**

19 - Ozone pollution degrades the components of floral odour plumes

20 - Reaction rates were fastest at the plume edges and slowest at the plume centre

21 - Exposure to higher ozone concentrations increased plume intermittency and
22   reduced odour filament width

23 - Honeybees recognition of floral odour plumes declined significantly following
24   exposure of the plume to ozone

25 **Graphical Abstract**
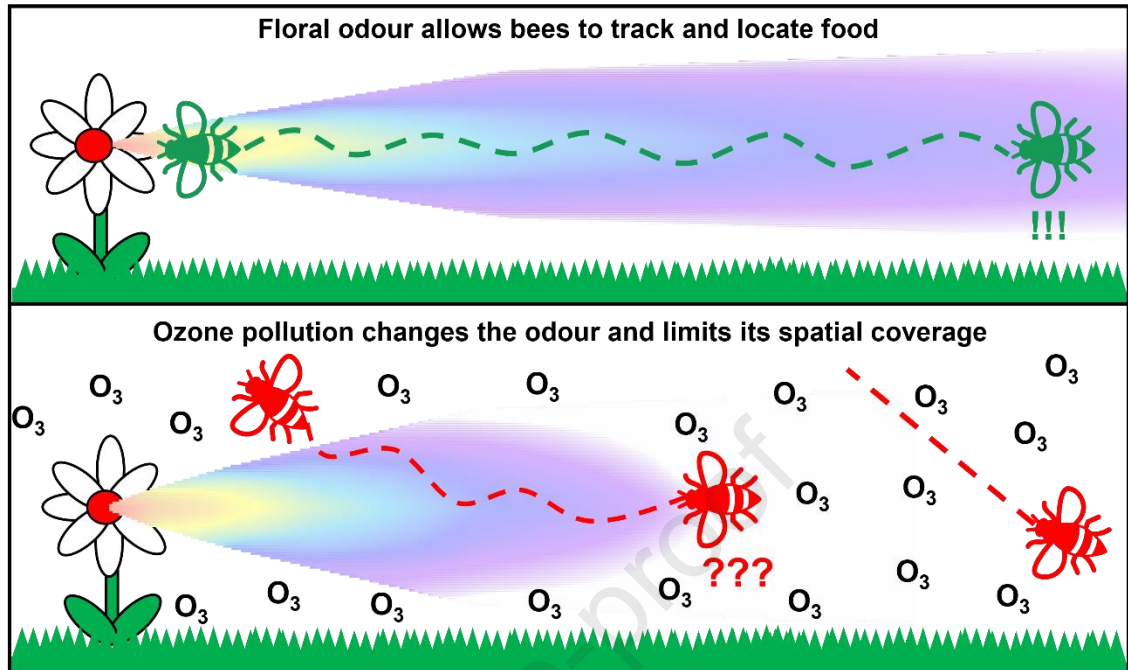
Abstract

The critical ecological process of animal-mediated pollination is commonly facilitated by odour cues. These odours consist of volatile organic compounds (VOCs), often with short chemical lifetimes, which form the strong concentration gradients necessary for pollinating insects to locate a flower. Atmospheric oxidants, including ozone pollution, may react with and chemically alter these VOCs, impairing the ability of pollinators to locate a flower, and therefore the pollen and nectar on which they feed. However, there is limited mechanistic empirical evidence to explain these processes within an odour plume at temporal and spatial scales relevant to insect navigation and olfaction. We investigated the impact of ozone pollution and turbulent mixing on the fate of four model floral VOCs within odour plumes using a series of controlled experiments in a large wind tunnel. Average rates of chemical degradation of α-terpinene, β-caryophyllene and 6-methyl-5-hepten-2-one were slightly faster than predicted by literature rate constants, but mostly within uncertainty bounds. Mixing reduced reaction rates by 8-10% in the first 2 m following release. Reaction rates also varied across the plumes, being fastest at plume edges where VOCs and ozone mixed most efficiently and slowest at plume centres. Honeybees were trained to learn a four VOC blend equivalent to the plume released at the wind tunnel source. When subsequently presented with an odour blend representative of that observed 6 m from the source at the centre of the plume, 52% of honeybees recognised the odour, decreasing to 38% at 12 m. When presented with the more degraded blend from the plume edge, recognition decreased to 32% and 10% at 6 and 12 m respectively. Our findings highlight a mechanism by which anthropogenic pollutants can disrupt the VOC cues used in plant-pollinator interactions, which likely impacts on other critical odour-mediated behaviours such as mate attraction.

2

1. Introduction

Floral odours are used by many pollinating insects to locate floral resources. Upon landing on a flower, many species of pollinating insect can learn to associate the unique blend of chemical compounds that make up the flower's odour profile with the nectar reward that it provides, facilitating them to locate rewarding flowers of the same species in the future (Jones and Agrawal, 2017). When an insect uses floral odours to locate a flower, that odour must fulfil certain criteria. For example, it must be relatively short lived, to ensure it does not accumulate, making the cue from individual flowers indistinguishable from the ambient background. At the same time, it must persist for sufficiently long to (i) reach insects and (ii) remain recognisable. Chemical communication is therefore a trade-off between short-lived cues with strong concentration gradients, and long-lived cues that travel further with weak concentration gradients (Williams and Ringsdorf, 2020).

Monoterpenes and sesquiterpenes are groups of volatile organic compounds (VOCs) which typically fulfil these criteria and are common components of floral odours (Knudsen et al., 2006).They have relatively short atmospheric lifetimes in the order of tens of minutes to several hours with respect to the hydroxyl radical (OH), the principal oxidant in the troposphere during the daytime, and with respect to NO_3 at night (Atkinson, 2000). Yet, these compounds can also be removed via reactions with ozone (O_3), a powerful oxidant formed at ground level when VOCs and oxides of nitrogen react in the presence of sunlight (Zhang et al., 2019). In the Northern hemisphere background concentrations of O_3 are in the range of 25 to 50 ppb and are further increasing at a rate of between 0.2 and 2% per year due to an increase in the emissions of its chemical precursors (Vingarzan, 2004), and local pollution episodes can see concentrations in excess of 200 ppb, particularly within or downwind of large conurbations (Group, 2021). For many monoterpenes and sesquiterpenes, reaction with O_3 is more efficient than reaction with OH, resulting in significantly shorter lifetimes. For example, α-terpinene has a lifetime of 45 minutes with respect to OH, but less than 30 s when O_3 concentrations exceed 70 ppb (Atkinson et al., 1986).

Reaction rates found in the literature assume complete mixing between VOC and oxidant, yet this may not be the case outside of the laboratory. This is particularly true for highly reactive compounds because their chemical lifetime is of the same order as the mixing time scale. This effect of spatial segregation between oxidant and VOC is often overlooked and our understanding of the applicability of reaction rates derived in a laboratory for use in the atmosphere is, therefore, uncertain.

An odour plume consists of a series of filaments, which can be considered as strands of higher concentrations of odour, that are formed by turbulent mixing. Recording VOC concentrations at any one stationary point in a plume as it moves and shifts with air movements would reveal bursts of high concentration as a filament is encountered, in-between absences of VOC, defined as the intermittency of the plume (J Murlis et al., 1992). It is this intermittency of signal that an insect's antennae encounters as it attempts to navigate upwind through to the plume's source. The combination of the constituents of an odour plume and its structure are both critical in influencing an insect's in-flight behaviour, enabling it to successfully navigate to the odour source. For example, it is well understood that male moths follow the pheromone plume of a mate by modifying their behavioural responses as a result of the frequency at which they encounter individual odour filaments (Mafra-Neto and Cardé, 1994). Similarly, the plume structure and

101 intermittency of plant and flower odours is important in facilitating the navigation of insects
102 to those odour sources (Beyaert and Hilker, 2014; Riffell et al., 2014).

103   A recent field study using O_3 fumigation by Ryalls et al. (2022) found that the
104 number of pollinators visiting individual flowers declined by 89% when O_3 pollution was
105 elevated above ambient levels. One explanation for this decline was that elevated O_3 may
106 have rapidly degraded components of the floral odour, inhibiting the ability of insects to
107 recognize this odour and successfully locate the flower. This hypothesis was supported
108 by the findings of a mesocosm study on the effects of ozone on the foraging behaviour of
109 the buff-tailed bumblebee, *Bombus terrestris* (Saunier et al., 2023). A second
110 complementary theory, is that air pollutants also cause direct oxidative stress on the
111 insect; studies have demonstrated upregulation of proteins associated with learning and
112 memory in the CNS of honeybees (Reitmayer et al., 2022) and olfactory coding
113 impairment (Démares et al., 2022). It is therefore likely that both mechanisms play a part.

114   However, there is a gap in the mechanistic empirical evidence to explain how VOC
115 odour degradation by O_3 occurs within an odour plume at temporal and spatial scales
116 relevant to insect navigation and olfaction. To assess the impact of O_3 on the degradation
117 of floral odour plumes a series of experiments were undertaken in a 20 m wind tunnel,
118 modified to allow fumigation by O_3 to predefined levels. The study focused on four VOCs,
119 α-terpinene, β-caryophyllene, 6-methyl-5-hepten-2-one (MHO) and linalool, which are all
120 common components of floral odours (Knudsen et al., 2006), represent a range of
121 atmospheric lifetimes, and have different molecular weights so are distinguishable from
122 one another in real-time using a proton transfer reaction time-of-flight mass spectrometer.
123 Here, we present the results for both a single compound odour plume (α-terpinene) and
124 multicomponent odour plumes (α-terpinene, β-caryophyllene, MHO and linalool) under O_3
125 concentration fields of approximately 0, 50 and 150 ppb. The measured odour plumes are
126 compared against those expected based on literature rate constants at various points
127 within the plumes.
128 In addition, a separate behavioral assay was conducted to assess whether the
129 degradation of odour plumes could affect the ability of honeybees to recognise an odour.
130

131 **2. Materials and methods**

132

133 **2.1   Wind tunnel measurements**

134   Measurements were made at the Natural Environment Research Council
135 (NERC) and National Centre for Atmospheric Science (NCAS) wind tunnel facility at the
136 University of Surrey. The Environmental Flow (EnFlo) wind tunnel is a 20 m (L) x 1.5 m
137 (H) x 3.5 m (W), draw down design with the capability of modulating inlet flow temperature
138 and generating specific boundary layer conditions (Carpentieri et al., 2012),(Hancock and
139 Pascheke, 2014). Within the tunnel are two three-dimensional traversing gears, which
140 allow the automation of sampling at specific, predefined locations. The tunnel is equipped
141 with a gas handling system to enable the passive release of trace gases at predefined
142 locations within the tunnel. The first seven meters of the tunnel are used to establish
143 boundary conditions and mixing, leaving approximately 12 m of wind tunnel to perform
144 measurements, with the final 1 m inaccessible to the 3D traverse.

145   A nominally 1 m deep boundary layer was generated in the wind tunnel, using a
146 standard system of triangular spires (Irwin, 1981) and a rough surface. Previous work had
147 established the characteristics of this boundary layer, including the variation of mean
148 velocity, turbulence intensity and turbulence length scales with height. The experiments

4

149 used two separate release heights, 0.5 and 0.75 m. Lateral and vertical turbulence
150 intensities at the two heights were 4.5 % and 3.2 % for the vertical component and 5.2%
151 and 3.2 % for the lateral: length scales were similar at the two heights being 11% of the
152 boundary layer height of ~ 1 m for the vertical component and 13% for the lateral
153 (Carpentieri and Robins, 2015). Finally, we note that these heights are well above the
154 near-wall, logarithmic region, which extends top about 20% of the boundary layer depth.
155 Further rationale for the wind tunnel setup is given in Section 1.1 of the Supplementary
156 Information (SI).

157

2.1.1 Ozone Fumigation

159 The concentration of O_3 inside the wind tunnel was controlled by releasing O_3 from
160 a lattice manifold, which was suspended in front of the upwind air intake of the wind tunnel.
161 The lattice comprised 35 mm diameter PVC tubing to form a 3.5 m by 1.5 m rectangle with
162 four vertical struts at regular (0.67 m) intervals. The tubing had 5 mm diameter holes drilled
163 at 25 mm intervals to allow for an even distribution of the O_3 into the tunnel. The O_3
164 concentration inside the wind tunnel was continuously monitored (2B Technologies, Model
165 202 Ozone Monitor) at a fixed location (see Fig. 1a) with the measured concentration used
166 to feedback to a Proportional–Integral–Derivative (PID) controller which in turn determined
167 the release rate of O_3 from two generators (CD1500P, ClearWater Tech, USA). Working
168 section O_3 levels only reached target concentrations when the entire laboratory that
169 houses the wind tunnel reached steady-state conditions. Two O_3 levels were used: ~50
170 ppb during the working-day, based on the ambient air quality standard (60 ppb), and 150
171 ppb at other times, based on the work-place standard (200 ppb). For this reason, the main
172 fumigation experiments were conducted outside of working hours to avoid exposing
173 laboratory users to concentrations exceeding the air quality standard. High frequency (10
174 Hz) measurements were also made using an O_3 monitor (Ecophysics, CLD 88 O_3) and
175 both analysers were calibrated against an O_3 calibration source (2B Technologies, Model
176 306).

177

2.1.2 Simulated floral odour plumes

179 Floral odours were simulated by releasing a blend of five trace gases which
180 ensured consistency throughout and between experiments. These included propane, an
181 inert tracer compound with respect to O_3 (Atkinson, 2000) and four VOCs, α-terpinene, β-
182 caryophyllene, MHO and linalool. Propane was released directly from a gas cylinder,
183 whereas the remaining four compounds were generated using a custom-built diffusion
184 device. Liquid standards of the four compounds were sealed in stainless steel (316 grade)
185 diffusion tubes and placed into one of two stirred water baths (Grant Instruments, TX150,
186 Cambridge). Oxygen free nitrogen was passed through a zero air generator (ZA FID AIR
187 6.0, Uvison Technologies, UK) and then flowed over the diffusion tubes at a rate of 0.3 L
188 min^{-1}. The VOC rich air was subsequently combined with propane (UN1978 Propane,
189 Tech Grade N1.5) and released through a ¼" diameter (O.D.) isokinetic release nozzle at
190 a flow rate of 1 L min^{-1}. This release rate ensured the simulated floral odour exited the
191 manifold at the same velocity as the air in the wind tunnel (~0.7 m s^{-1}) ensuring a passive
192 release of the VOCs. The concentration of each VOC closest to the release point (x, y

coordinates of 0.5, 0 m, see Fig. 1b) was ~100 ppb for α-terpinene, 6 ppb for β-caryophyllene, 2.5 ppb for Linalool and 4.5 ppb for MHO.
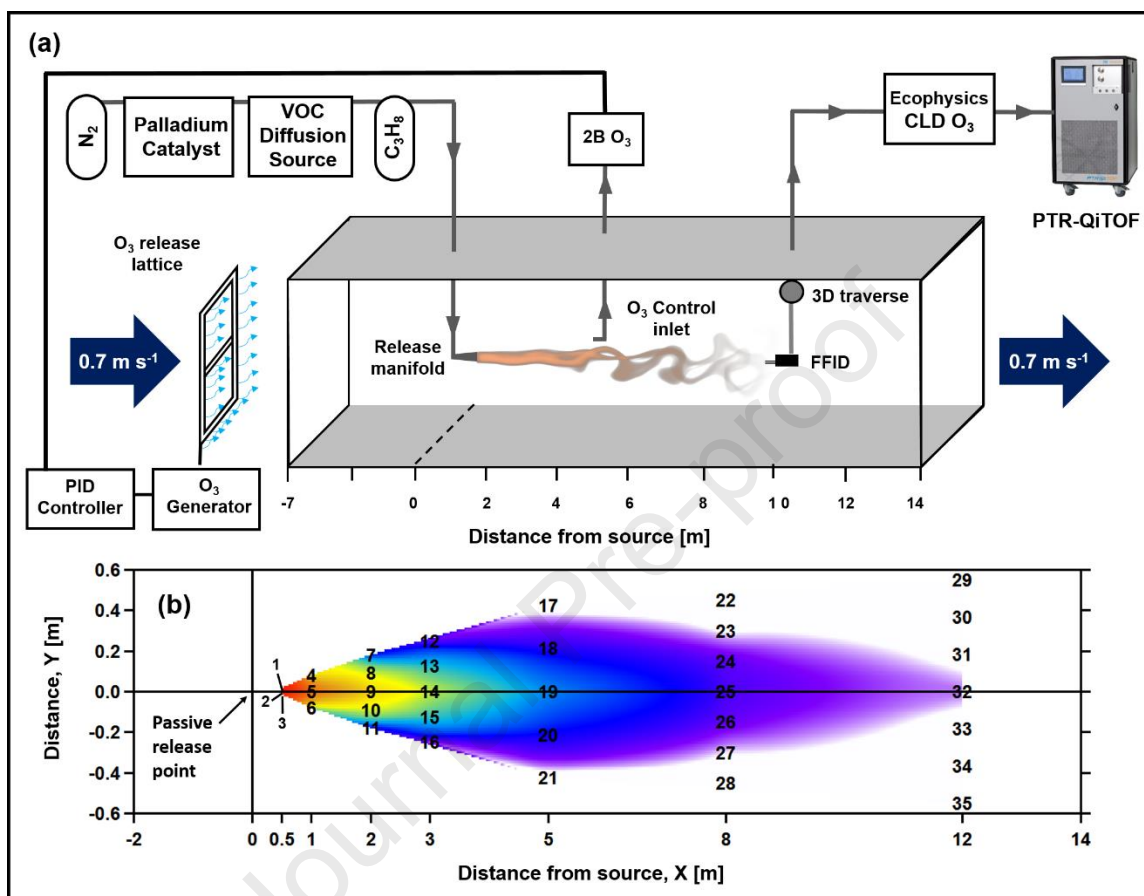
Figure 1. Schematic of the wind tunnel measurement setup (panel a) and cross-section of the wind tunnel identifying the positions of the 35 measurement locations used (panel b).

2.2   Measurement of floral odour

2.2.1 Proton transfer reaction – time-of-flight – mass spectrometer

The concentration of the VOCs within the simulated floral odour were measured using a proton transfer reaction time-of-flight mass spectrometer, with quadrupole ion guide (PTR-QiTOF, Ionicon Analytik GmbH, Austria) (Jordan et al., 2009). The conditions within the instrument's drift tube were kept constant throughout each experiment with pressure, temperature and voltage maintained at 3.8 mbar, 80 °C and 860 V, respectively. This ensured the ratio between electric field and number density of molecules (*E/N*) within the drift tube was maintained at 122 Td and that fragmentation of ions remained consistent. An assessment of ion fragmentation and instrument calibration is shown in Section S1.2 of the SI.

6

211   Air was sampled from the wind tunnel at a rate of ~ 6 L min^{-1} (at 500 mbar) from a
212 ~25 m long ¼" O.D (1/8" I.D) PFA sampling line. To avoid sampling at reduced pressures,
213 air for analysis by PTR-QiTOF was subsampled using a Teflon headed pump (KNF) to
214 pass the air past the instrument inlet. The sample line was mounted directly to the three-
215 dimensional traverse inside the wind tunnel and the tube heated to 80 °C to limit absorption
216 of VOCs to the tube walls. A PTFE filter (0.45 µm pore size) was placed in line after the
217 pump to prevent particulate matter entering the instrument. The temperature of the air
218 within the sample line was monitored continuously and was to within 1 °C of the recorded
219 wind tunnel temperature.

220   A Fast Flame Ionisation Detector (FFID, Cambustion, HFR400) was used
221 to provide highly time resolved measurements of the plume structure. The frequency
222 response of the FFID is 200 Hz and is small enough to be mounted on the traverse. The
223 FFID operates in the range of 1000 to 0.05 ppmv. Air was sampled into the FFID along a
224 350 mm length of steel tubing (O.D. = 0.55 mm). The FFID was calibrated at the start of
225 the experiment and frequent background measurements were made to allow for drift
226 corrections   which   were   on   average   less   than   3%.
227

2.2.2 *Sampling Protocol*

229   Each plume was sampled at 35 separate locations comprising seven horizontal
230 cross sections at 0.5, 1, 2, 3, 5, 8 and 12 m downwind of the release point (Fig. 1b). Direct
231 measurements at point 0, 0 (co-ordinates are distances x, y in m relative to the release
232 point and height) were not feasible and therefore measured concentrations at each
233 location in the wind tunnel were always normalised to the 2nd measurement point (e.g. x =
234 0.5 m, y = 0 m), which became the effective release point.

235   PTR-QiTOF data were recorded with a time resolution of 10 Hz and sampled at
236 each of the pre-defined locations for 13 minutes. This duration was found to offer a good
237 compromise between obtaining robust statistics and ensuring all measurement locations
238 could be sampled during the time period when O$_3$ fumigation in the laboratory was
239 permitted. Following each wind tunnel measurement, the background concentration was
240 monitored by sampling at the wind tunnel edge, outside of the plume for 1 minute. The
241 final step was to measure the concentration of VOCs coming from the diffusion source for
242 1 minute, to ensure any minor deviations in release concentration could be corrected. In
243 total, each plume characterisation experiment took approximately 9 hours to complete.

2.3   Plume intermittency and odour filament width

245   The intermittency of an odour plume is defined here as the fraction of time (0-1)
246 the VOC concentration falls below the threshold of perception (ToP). This threshold is
247 insect dependent, so here an arbitrary value defined as 1% of the 98th percentile of
248 observed concentrations was used. The width of individual odour filaments was calculated
249 by counting the number of consecutive measurements falling below the ToP at each
250 location within the wind tunnel and averaging the results. The sampling rate of the PTR-
251 QiTOF was 10 Hz and, therefore, each measurement was equivalent to a filament width
252 of 0.1 s.

2.4   Proboscis extension response assay

254   To establish the effects of O_3 induced changes to the composition of floral odours
255   on a pollinating insect's ability to successfully recognise that odour, proboscis extension
256   response (PER) assays were performed using the western honeybee (*Apis mellifera*).

257   Liquid standards of the four VOCs used in the wind tunnel study were mixed into
258   a blend, with volumes initially based on the vapour pressure of each compound (Table
259   S1). Concentrations were assessed using a solid phase microextraction fibre (SPME) in
260   combination with GC-MS and the methods used are outlined in Section 1.3 of the SI.
261   Having established the initial ratio of the blend, two sets of three further odour blends were
262   prepared aiming to replicate the ratios observed in the wind tunnel under the 150 ppb
263   treatment at distances of 2, 6 and 12 m from the source. The first set represented the
264   ratios seen in the plume centre and the second represent those seen at the plume edge.
265   SPME collection and GC/MS analysis were repeated on two random blends to ensure that
266   individual compounds were within 2% of the calculated fractions.

267   Proboscis Extension Response assays were conducted in an air-conditioned room
268   at ca. 21 °C, lit by artificial light, with O_3 concentrations always at background levels (<10
269   ppb (Nazaroff and Weschler, 2022)). Returning forager honeybees were collected from
270   the entrance of a hive maintained on the University of Reading's Whiteknights campus
271   (51° 26' 9" N, 0° 56' 25" W). Individual worker bees were immobilised by cooling them on
272   ice in 60 mL containers before being transferred and harnessed into a 1 ml pipette tip
273   (Felsenberg et al., 2011). Only honeybees showing an initial PER elicited by 1.5 M sucrose
274   solution were used. Each honeybee was trained to associatively learn the source VOC
275   blend (α-terpinene, β-caryophyllene, MHO and linalool in a 1:1:1:1 ratio). Following the
276   protocol of Matsumoto et al. (2012), honeybees were acclimatised to a continuous flow
277   (650 mL min^{-1}) of charcoal-filtered humidified air for 25 s before being presented with the
278   4 s conditioned odour stimulus (i.e. an odour stream from a glass pipette containing filter
279   paper impregnated with 20 μL of the source blend). This was immediately followed by a 3
280   s sucrose stimulation (unconditioned stimulus; 1.5 M sucrose solution) with a 1 s overlap,
281   regulated by a CS-55 V2 stimulus controller (Syntech, The Netherlands). Honeybees were
282   left in the air stream for a further 25 s after sucrose delivery to ensure that no contextual
283   cues around the setup would be associated with the unconditioned stimulus. Honeybees
284   were scored as having learnt the source blend if a proboscis extension was observed
285   between odour onset and sucrose delivery. The learning trial was repeated four times for
286   each honeybee and the inter-trial interval for each honeybee was 10 min. In the
287   recognition trials the responses of 77 honeybees were tested to each of the six odour
288   blends that had been prepared to replicate the VOC ratios recorded in the wind-tunnel
289   experiments at either 2, 6 or 12 m from the source at either the plume centre or the plume
290   edge. Recognition trials mirrored the conditioning trials, with the omission of sucrose.
291   Extension of the proboscis within 4 s in response to the onset of the odour stimulus was
292   classified as a positive recognition. The procedure was followed by the presentation of the
293   source blend (0 m). Honeybees that did not extend their proboscis in response to the final
294   conditioned stimulus (N = 6 of 77) were excluded from analysis. As such, 34 and 37
295   individuals responding to VOC blends at the plume centre and plume edge, respectively
296   (71 honeybees in total), were incorporated in statistical analyses (see Section 1.4 of the
297   SI).

298

299

3. Results and discussion

3.1 Wind tunnel plume measurements

3.1.1 α-terpinene plume

A single component release of α-terpinene was used to map out the spatial distribution of an odour plume and to determine how this changed under differing levels of O_3 pollution. Figure 2 shows the measured odour plumes under O_3 fields of 0 (Fig. 2a), 50 (Fig. 2b), and 150 ppb (Fig. 2c). Background O_3 levels within the wind tunnel were between 8 and 12 ppb and therefore a true 0 ppb field could not be achieved. Instead, Fig. 2a shows a plume of propane, which does not react with O_3 and can therefore be considered representative of the α-terpinene plume injected into a zero O_3 concentration field.

310

311
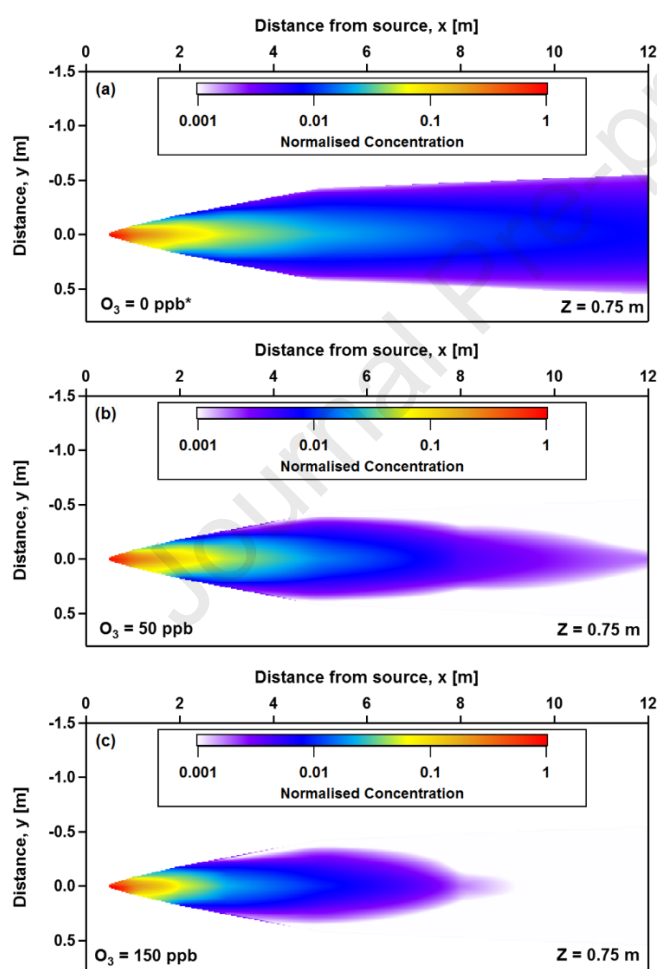
Figure 2. Horizontal plume cross sections showing the concentration of α-terpinene normalised to the point closest to the odour plume source for ozone (O_3) fields of ~0 (panel a), ~50 (panel b) and ~150 ppb (panel c). The colour scale of each plume has been log normalised. * Panel a shows a plume of propane, which does not react with O_3 and can, therefore, be considered representative of the α-terpinene plume injected into a zero O_3 concentration field.

317

318   Each plot consists of the 35 individual measurement points (shown in Figure 1b)
319 which have subsequently been interpolated using the "natural neighbour" approach and
320 Voroni tessellation (See "image_interpolate" function, Igor Pro, Version 8.0.3.3,
321 Wavemetrics). Similar plots showing the average O_3 concentration are shown in the
322 Supplementary Information (figure S1).

323   For each experiment the wind tunnel was operated using a standard 1 m boundary
324 layer. which resulted in a wind speed of 0.68 m s^{-1} at the 0.75 m height and 0.63 m s^{-1} at
325 the 0.5 m measurement height, equivalent to travel times of ~16.9 and 18.25, respectively,
326 between the effective release point and the end of the wind tunnel. Figure 2a, where no
327 ozonolysis occurs, demonstrates the effect of dilution on the plume, concentrations
328 dropping to < 1% of the effective release point by the time the air exits the wind tunnel.

329   The addition of O_3 to the wind tunnel changed the plume shape causing a
330 narrowing as the α-terpinene mixed with the O_3 rich air at the plume edges. Figure 2b
331 shows that ozonlysis removed almost all of the α-terpinene in the 16 s that it took for plume
332 to travel the length of the wind tunnel at 50 ppb of O_3, and at 150 ppb (Fig. 2c), all of the
333 α-terpinene had reacted away by 9.5 m (13.5 s). These two-dimensional cross sections
334 demonstrate how a plumes spatial extent, both length and width, can be significantly
335 reduced under increasing levels of O_3 pollution at concentrations regularly observed in the
336 lower troposphere at background levels (50 ppb) and also during elevated pollution
337 episodes (150 ppb) (Group, 2021).

338   The α-terpinene plumes were also modelled by subtracting the expected chemical
339 loss from the conserved propane plume. Theoretical first-order loss rates were calculated
340 as

341
$$Loss = \left(\frac{t}{t_{loss}}\right), \tag{2}$$

342 where t is the time since release into the O_3 field in seconds and t_{loss} is the total
343 loss rate of VOC with respect to O_3 calculated as

344
$$t_{loss=}\left(\frac{\left(k_{AT,O_3}\right)^{-1}}{[O_3]}\right). \tag{3}$$

345   Here, $k_{AT,O3}$, is the ozonolysis rate constant (see Table S1) and [O_3] was the
346 concentration of O_3 measured at each location in the wind tunnel in molecules cm^{-3}. The
347 time since release was calculated based on the straight-line distance between the
348 effective release and measurement point and the fixed wind speed.

349   Figure 3, panels a and b show the percentage difference between measured and
350 theoretical plumes for the ~50 and ~150 ppb O_3 fields, respectively. In both cases, the
351 measured plume is degraded more quickly than would be expected based on the literature
352 rate constant: an average of 21% for 50 ppb and 24% for 150 ppb, based on the measured
353 data points, only. This was partially explained by the additional time available for reaction
354 as sampled air was drawn into the PTR-QiTOF. A cross-covariance function applied to the
355 propane signal measured *in situ* by the FFID (and used for the theoretical plume
356 calculations) and PTR-QiTOF showed this delay to be ~1.6 s (see Figure S2 of the SI).

357   Accounting for this additional delay reduced the average difference to 18% and 12%, for
358   50 ppb and 150 ppb scenarios, respectively.

359   The overall increased reaction rates may be influenced by additional chemical
360   sinks in the wind tunnel including reactions with either OH or NO_3, which were not
361   measured during the study. The spatial behaviour of the plume supports the view that
362   imperfect mixing affects the rate constant: the difference plots highlight the increased
363   reaction rate at the plume edges, where mixing between O_3 and the VOC is particularly
364   efficient, but less change is seen at the plume centre. The reaction rate appears slowest
365   during the first 0.5 to 2 m after release, which is consistent with the limited opportunity for
366   mixing shortly after release. Incomplete mixing reflects the intensity of segregation
367   between the O_3 and VOCs,
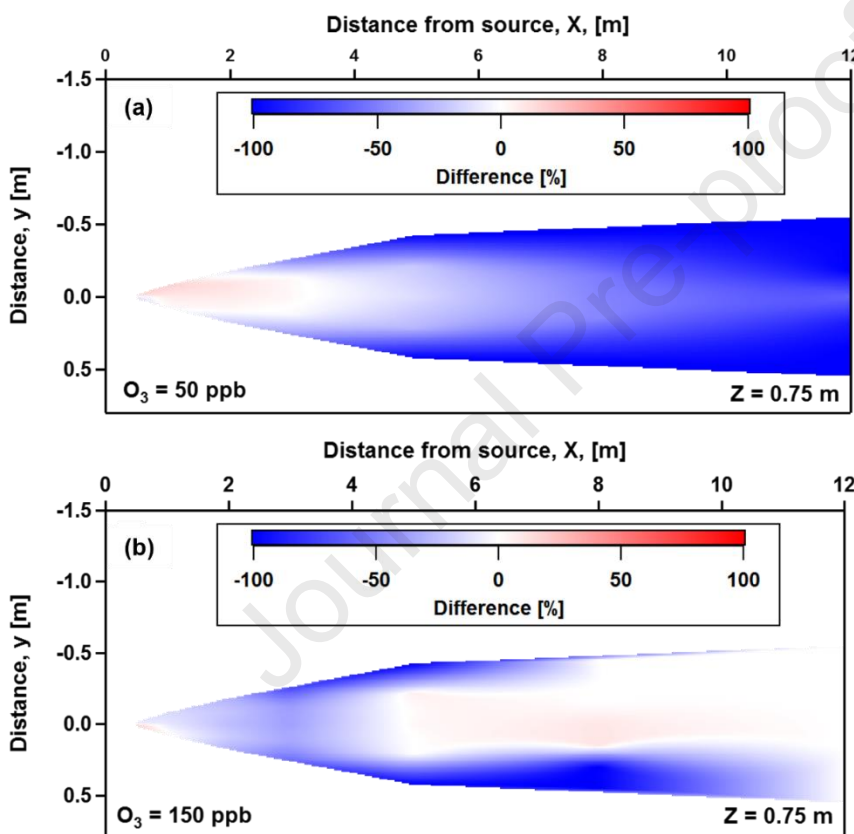
368
369   **Figure 3 shows the percentage difference between an a-terpinene plume predicted based on literature rate**
370   **constants and that measured by the PTR-QiTOF (e.g. measured – predicted)/predicted). Panel a and b show the**
371   **difference plot under ozone conditions of 50 ppb and 150 ppb of ozone, respectively. Both plumes were released**
372   **from a height of 0.75 m.**

373

374

375   which effectively reduces the rate constant and increases the lifetime of the compound.
376   The rate of change of VOC concentration with respect to O_3 can be calculated as

377     $$\frac{\partial [VOC]}{\partial t} = -k_{VOC,O3}([O_3][VOC] + [O_3'VOC']), \quad\quad\quad\quad (4)$$

11

378   where square brackets represent averages and the primes denote deviations from the
379   mean concentration. Using the measured α-terpinene and O_3 concentrations, both
380   measured at 10 Hz, the effective rate coefficient ($k_{eff,AT,O3}$) can be calculated following the
381   approach of Krol et al. (2000) and Pugh et al. (2010), where the intensity of segregation,
382   S, between O_3 and α-terpinene is defined as

383    $$S_{AT,O_3} = \frac{[O_3' AT']}{[O_3][AT]}.$$ (5)

384   This intensity of segregation can be used to derive an effective rate constant as:

385    $$k_{eff,AT,O3} = k_{AT,o_3}(1 + S_{AT,O_3}).$$ (6)

386   Figure 4, panel (a) shows the effective rate constant for α-terpinene, calculated
387   based on the α-terpinene plume released at a height of 0.75 m into an O_3 field of 150 ppb.
388   The literature rate constant for α-terpinene is 2.1 x 10^{-14} cm^3 $molecule^{-1}$ s^{-1}, and the
389   effective rate constant is roughly equivalent to this at the plume centre between 4 and 8
390   m. However, at the effective release point (y=0, x=0.5), $k_{eff,AT,O3}$ is decreased by ~8%,
391   thereby increasing the lifetime of α-terpinene at that point. Towards the plume edges, from
392   3 m down the tunnel and beyond, $k_{eff,AT,O3}$ is closer to k_{AT}, than at the plume centre where
393   there the α-terpinene has less opportunity to mix with the O_3.

394   Repeating the same experiment at the lower height of 0.5 m (Figure 4b), where
395   turbulence is slightly increased, showed a somewhat steeper gradient in the effective rate
396   constant, with up to a 10% reduction at the effective release point. This is counter to
397   expectation because the increased turbulence and longer travel time should enhance
398   mixing and reduce the effects of segregation. Figure 3c shows the effective rate constant
399   for both measurement heights at each location within the tunnel. There is a small
400   difference between the effective rate constants measured at 0.5 and 1 m but this was
401   within the uncertainty bounds which was based on the standard deviation of the
402   measurements. This potentially reflects the fact that differences in the turbulence
403   intensities between the two heights was relatively minor (4.5 % and 3.2 % for the vertical
404   component and 5.2% and 3.2 % for the lateral). Further measurements at lower heights
405   were not possible due to the potential for the plume to interact with the wind tunnel's
406   surface.

407   A maximum 8-10% decrease of the rate constant may appear modest, but it should
408   be viewed as a lower limit. This is because our instruments were limited to a frequency
409   response of 10 Hz. Comparison of the PTR-QiTOF measurements with those of propane
410   made by the FFID at a frequency of 200 Hz, revealed fine scale variation in concentration
411   that is lost when using a 10 Hz measurement (see Fig. S3). Therefore, the effects of
412   segregation could be greater; particularly for an insect encountering the plume, whose
413   antennae can detect changes at a rate far greater than 10 Hz (Szyszka et al., 2014).

414   This result indicates that mixing plays an important, but often overlooked, role in
415   the lifetime of VOCs. For those VOCs used as chemical cues, this is particularly important
416   because the short lifetimes necessary to generate strong concentration gradients mean
417   the lifetime of the signal compound is invariably similar to, or shorter than, the mixing time
418   scale.
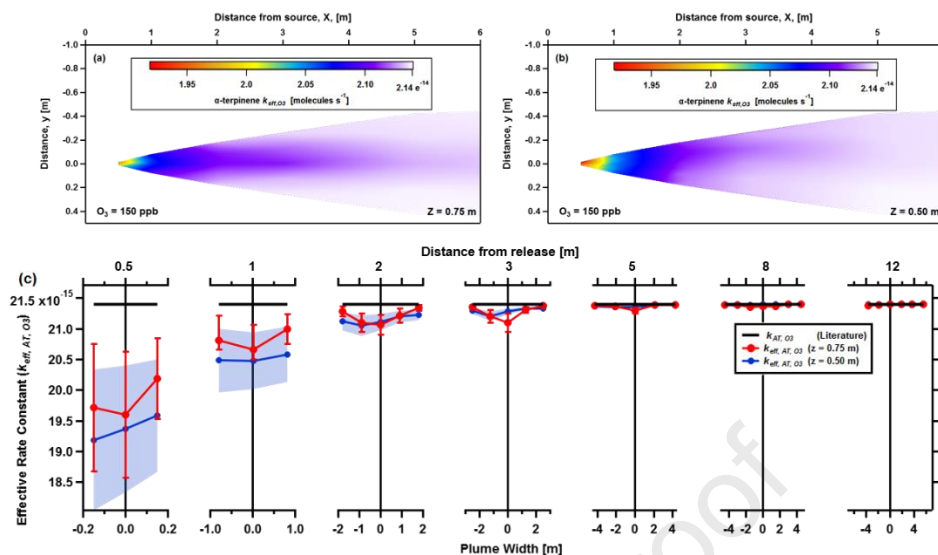
419

420　Figure 4. The effective rate constant ($k_{eff,O3}$) for α-terpinene measured at 0.75 m (panel a) and 0.5 m (panel b) above
421　ground level when released into an ozone field of 150 ppb. Panel c shows the measured effective rate constant at
422　each point within the wind tunnel at the two measurement heights together with the uncertainty (red line = 0.75 m,
423　blue line = 0.5 m). The literature rate constant, k_{O3}, is 2.14 x 10^{-14} (black line). Turbulence levels were 3-5% higher
424　both laterally and vertically for the 0.5 m height.

425

3.1.2 Multi-component plume

427　　　　Cross sectional plots of each individual component of the multicomponent release,
428　which is more representative of a floral odour plume, showed variations in the reaction
429　rates of the four VOCs: α-terpinene, β-caryophyllene, MHO and linalool (see Fig. S4 a-d).
430　The difference between the theoretical and measured plumes are shown in Figure 5 and
431　a more detailed comparison that incorporates the uncertainty of the literature rate
432　constants is shown in Figures S5-S8. For α-terpinene, β-caryophyllene and MHO, the
433　measured plumes are again degraded faster than would be expected based on their
434　respective O_3 rate constants, with the largest differences occurring at the plume edge.
435　Applying a correction for the additional sampling delay accounted for 7% and 4% of the
436　difference for α-terpinene, β-caryophyllene, respectively, and less than 1% for MHO. As
437　was the case for a-terpinene, the reason for the reaction rates exceeding those expected
438　based on literature rate constants, even despite the effects of segregation, likely relates
439　to the presence of OH and or NO_3 within the wind tunnel.

440　　　　Linalool is degraded more slowly than implied by its rate constant and the
441　difference becomes larger towards the plume edge. It is likely that an oxidation product,
442　from either α-terpinene or β-caryophyllene is formed which contributes to the linalool
443　signal, most likely as a fragment ion. This is supported by the fact that the difference is
444　largest at the plume edge where the mixing and hence reaction rates are at their fastest.

445
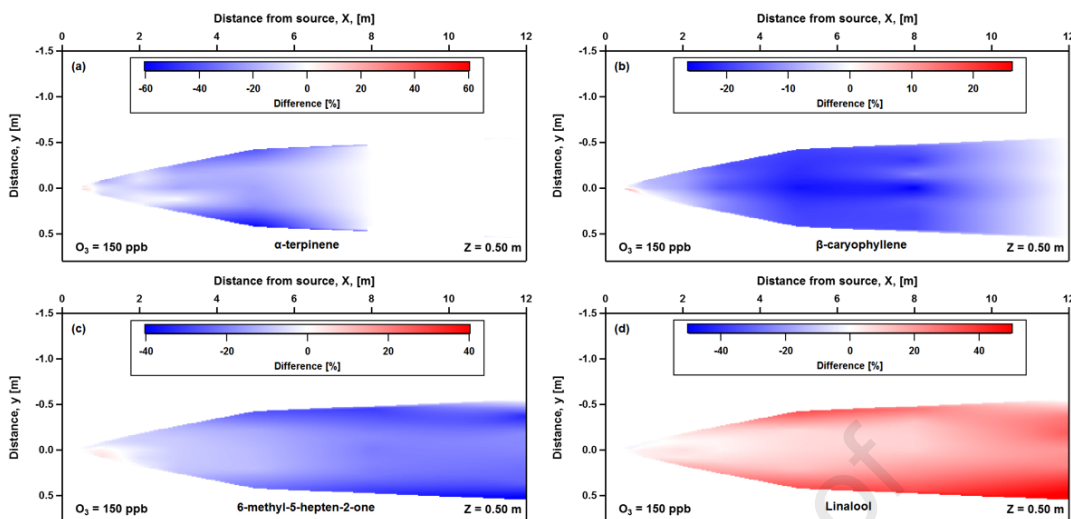
Figure 5 shows the percentage difference between VOC plumes that has been predicted based on literature reaction rates with O_3, and that measured by PTR-QiTOF (e.g. (measured – predicted)/predicted) Panel a-d show the results for a-terpinene (a), b-caryophyllene (b), MHO (c) and linalool (d). The odour plume was released from a height of 0.5 m into an ozone field of 150 ppb.

3.2   Effect of ozone on plume intermittency and odour filament width

Plume intermittency is considered to be a function of source strength and turbulent mixing. Yet. Figure 6 shows that higher levels of O_3 caused an increase in intermittency and reduction in odour filament width of an α-terpinene plume when released under identical turbulent profiles. These changes are likely to have behavioural consequences for a flying insect using the odour plume to navigate to a source. Both factors are critical in eliciting insect flight behaviours and small changes to plume structure can have dramatic effects on flight behaviour and the ability of a foraging insect to locate an odour source (Beyaert and Hilker, 2014; Mafra-Neto and Cardé, 1994) However, we did not directly investigate the effects of the changes we observed to intermittency and filament number on insect flight behaviour and therefore the degree of impact of those changes remains unclear. Again, the largest changes in intermittency and odour filament width were observed towards the outer edges of the plume where mixing with O_3 is most efficient.

14

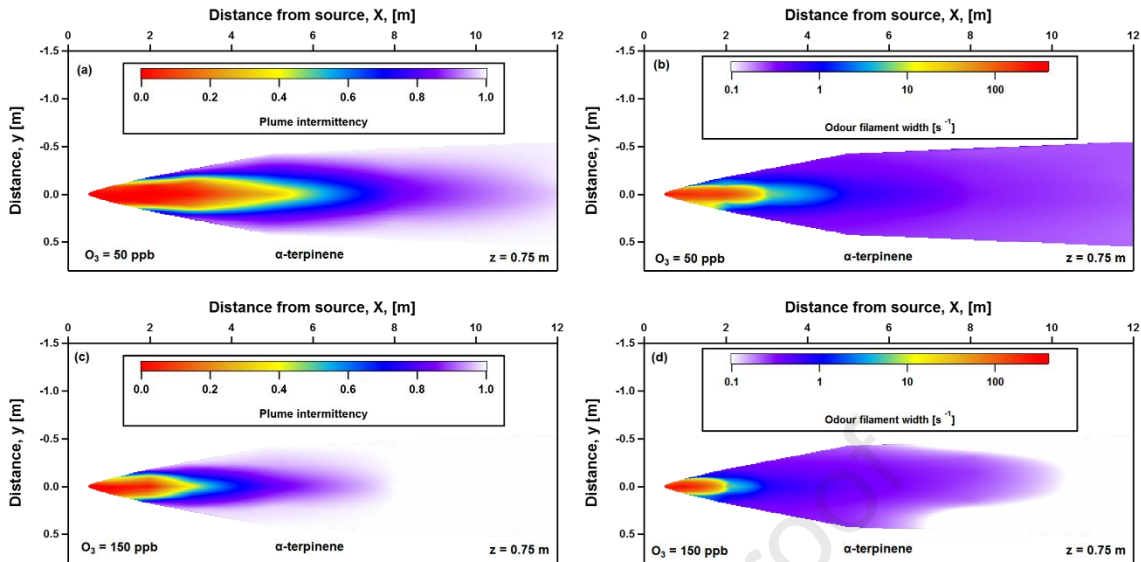Figure 6, panels a and c, show the intermittency of an a-terpinene plume, defined as the fraction of time (0-1) that the measured signal fell below the threshold of perception (see text for definition), under identical turbulent conditions but varying ozone concentrations of 50 ppb and 150 ppb, respectively. Panels b and d show the average odour filament width from the same a-terpinene plumes. Note the colour scale in panels b and d are shown on a logarithmic scale.

3.3 Honeybee Proboscis Extension Response (PER) Assays

Figure 7 shows the ratios recoded in the wind-tunnel under 150 ppb of O_3, and those reproduced for the PER assays. Panels a versus c show the plume centre and b versus d show the plume edge. The ratios were not identical but provided a reasonable approximation of the composition change observed in the wind tunnel.

When honeybees were presented with the VOC odour profile they had been trained to (i.e. the profile representative of the VOC blend at the tunnel source, or 0 m), 100% showed a positive PER response (Figure 7 c and d), i.e. all individuals recognised the blend to which they had been trained. However, for the less degraded central plume (figure 7 c), when honeybees were presented with a VOC blend representative of that recorded at 6 m from the tunnel odour source only 52% of honeybees tested exhibited a positive PER response, decreasing to 38% for bees presented with the VOC blend representative of 12 m from the odour source. For the honeybees presented with VOC blends representing the more degraded plume edge (Figure 7 d), just 32% responded to that representing 6 m from the odour source, decreasing to 10% to the blend representing 12 m from the odour source. Overall, significantly fewer honeybees responded to the VOC blend at the plume edge compared with the plume centre (χ^2_1 = 9.56, P = 0.002) and significantly fewer honeybees responded as the distance from the source increased (χ^2_1 = 39.17, P < 0.001). There was no significant two-way (Location x Distance) interaction (χ^2_1 = 9.56, P = 0.002. These results suggests that changes in VOC ratios resulting from O_3 pollution and at fairly small foraging distances from a floral odour source could cause large reductions in the ability of honeybees to be able to recognise a floral blend, potentially disrupting the processes pollinating insects rely on for location of floral food resources. This supports previous findings of behavioural studies, which have

15

502 demonstrated changes in insect behaviour (Vanderplanck et al., 2021) (Saunier et al.,
503 2023) and reduced pollination of flowers under elevated O_3 (Ryalls et al., 2022).

504

505   It should be noted that this assay purely assessed the honeybee's abilities to
506 recognise the odour and therefore, the results do not capture any additional effects
507 associated with direct exposure to O_3. Furthermore, here the honeybees are responding
508 to a mean concentration, and therefore, the additional impact of O_3 on the spatial extent
509 and intermittency of the plume as well as the odour filament width are not captured within
510 the honeybees response.

511

512

513
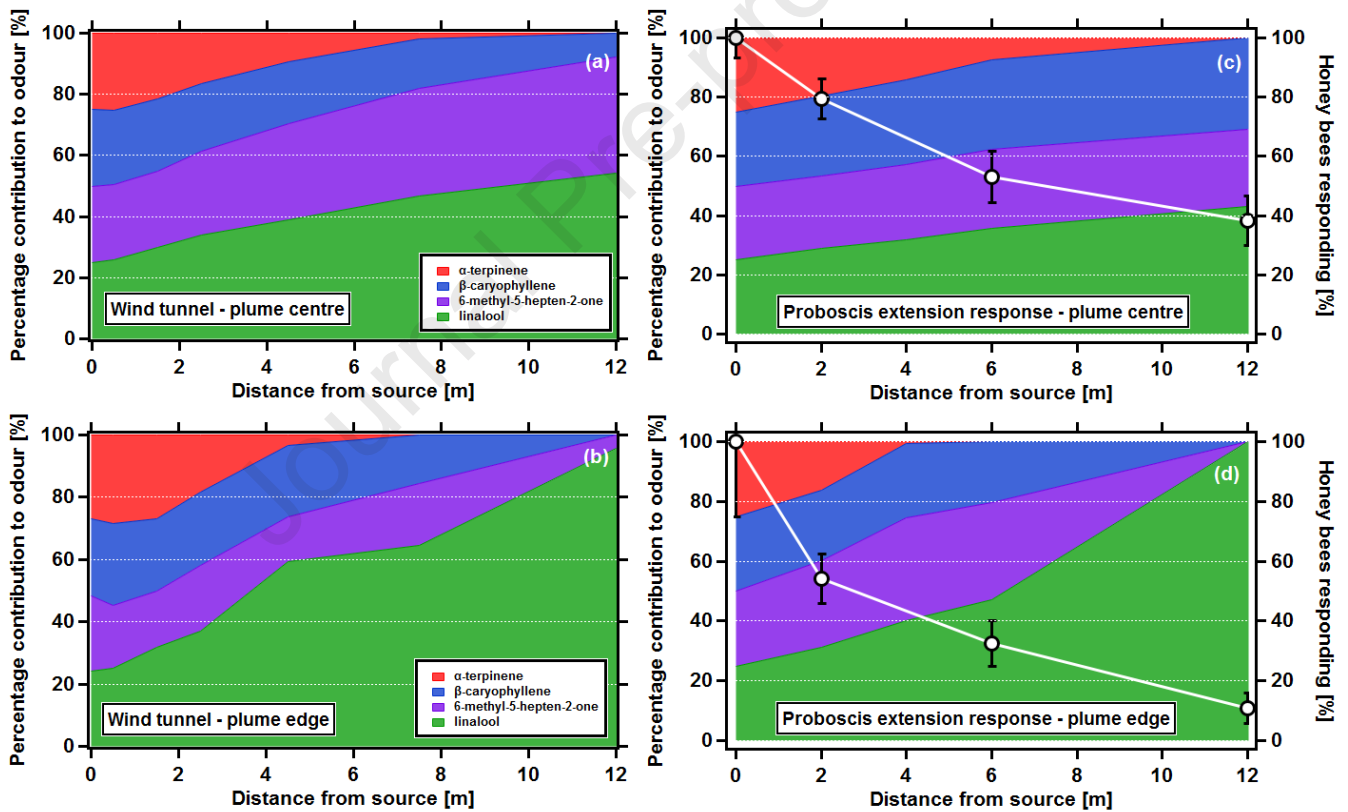
514
515 **Figure 7** Observed ratios of α-terpinene, β-caryophyllene, 6-methyl-5-hepten-2-one (MHO) and linalool measured at
516 the plume centre (panel a) and plume edge (panel b) under an ozone field of 150 ppb. Panels c and d show an
517 attempt to replicate these ratios as part of a proboscis extension response assay, for the plume centre and plume
518 edge, respectively. The right hand axis and line graphs on panels c and d indicate the percentage of forager
519 honeybees which, after learning the four VOC blend representative of 0 m from the source, extended their
520 proboscis (indicating recognition) when presented with VOC blends representative of 2, 6 and 12 m from the source
521 (± S.E.). Data are expressed as the percent PER recognition of each distance relative to the PER recognition of
522 blend at the source ((n = 34 and 37 individuals for the plume centre and plume edge, respectively). While there was
523 no significant two-way interactive effect of 'distance from the source' and 'location of the plume', both were
524 individually significant. As such, significantly fewer honeybees responded to the VOC blend corresponding to the

525 **plume edge compared with the plume centre (z = -2.814, P < 0.005) and honeybee responses significantly decreased**
526 **from 2 to 6 m (z = -3.39, P = 0.001) and from 6 to 12 m (z = -2.82, P = 0.005) according to post-hoc tests.**

527

4. Conclusions

529 Controlled releases of both single and multiple component synthetic floral odours
530 were measured in a wind tunnel under differing levels of O_3. The rate of reaction of each
531 compound (α-terpinene, β-caryophyllene, MHO and linalool) were found to be broadly
532 similar to that expected based on literature rate constants, but in most cases slightly faster,
533 likely due to additional chemical sinks (e.g. OH and NO_3) for the VOCs within the wind
534 tunnel. The notable exception was linalool, where reaction rates were slower than
535 expected. In this case, fragmentation of an oxidation product to *m/z* 155 was thought to
536 be the most likely cause.

537 An analysis of the intensity of segregation between the concentrations of α-
538 terpinene and O_3 revealed that the effective rate constant ($k_{eff,AT,O3}$) was reduced by up to
539 10% in the first 2 m following release. The effect of segregation was expected to decrease
540 at lower measurement heights, but no statistically significant difference was observed
541 between the 0.75 and 0.5 m measurements. This reflected the small differences in
542 turbulence intensity between these two measurement heights. Reaction rates were fastest
543 at the plume edges attributed to the increased opportunity to mix with ozone. Ozone was
544 also found to increase the intermittency of the plume and decrease odour filament width,
545 two properties used by insects for navigation.

546 Replication of the average plume composition in a proboscis response assay
547 clearly showed a rapid decline in honeybees' ability to recognise the floral odour following
548 simulated degradation by O_3. These results, although based upon a synthetic odour,
549 provide an important insight into the mechanism by which anthropogenic pollutants can
550 disrupt the chemical cues used by insects. Importantly, our experimental approach, where
551 the effects of O_3 degradation were replicated and then presented to the insect, allows its
552 effects to be de-coupled from potential olfactory coding impairment caused by direct
553 oxidative stress. In this instance, the effects are pronounced within just a short distance
554 from the point of release.

555 However, outside of the laboratory, the extent to which ozonolysis impacts on
556 pollinators will ultimately depend on the reactivity of the components within a given floral
557 odour, the ambient O_3 concentration (and NO_3 if at night-time) and wind speed.
558 Nonetheless, our work demonstrates a clear mechanism, capable of explaining the large
559 decline in pollinator visits seen in previous field scale O_3 fumigation studies (Ryalls et al.,
560 2022) which may also be relevant for other odour-mediated behaviours such as mate
561 attraction.

562

567
568
569

Declaration of competing interest
The authors declare that they have no known competing financial interests or personal relationships that could have appeared to influence the work reported in this paper.

Data availability

Data is available upon reasonable request.

Author statement

RG, BL, CP and EN obtained the funding, BL, NJM, DT, RG, CP, EN, PH and AR performed the wind tunnel study. JR, LB and RG performed the proboscis extension response assays and all authors contributed to the writing of the manuscript.

References

Atkinson, R., 2000. Atmospheric chemistry of VOCs and NOx. Atmospheric Environment 34, 2063-2101.

Atkinson, R., Aschmann, S.M., Pitts Jr., J.N., 1986. Rate constants for the gas-phase reactions of the OH radical with a series of monoterpenes at 294 ± 1 K. International Journal of Chemical Kinetics 18, 287-299.

Beyaert, I., Hilker, M., 2014. Plant odour plumes as mediators of plant-insect interactions. Biol Rev Camb Philos Soc 89, 68-81.

Carpentieri, M., Hayden, P., Robins, A.G., 2012. Wind tunnel measurements of pollutant turbulent fluxes in urban intersections. Atmospheric Environment 46, 669-674.

Carpentieri, M., Robins, A.G., 2015. Influence of urban morphology on air flow over building arrays. Journal of Wind Engineering and Industrial Aerodynamics 145, 61-74.

Démares, F., Gibert, L., Creusot, P., Lapeyre, B., Proffit, M., 2022. Acute ozone exposure impairs detection of floral odor, learning, and memory of honey bees, through olfactory generalization. Science of the Total Environment 827, 154342.

Felsenberg, J., Gehring, K.B., Antemann, V., Eisenhardt, D., 2011. Behavioural pharmacology in classical conditioning of the proboscis extension response in honeybees (Apis mellifera). J Vis Exp.

Group, A.Q.E., 2021. Ozone in the UK - recent trends and future projections, pp. 1-143.

Hancock, P.E., Pascheke, F., 2014. Wind-tunnel simulation of the wake of a large wind turbine in a stable boundary layer. Part 1: the boundary-layer simulation. Boundary-Layer Meteorology 151, 3+.

612   Irwin, H.P.A.H., 1981. The design of spires for wind simulation. Journal of Wind Engineering and
613   Industrial Aerodynamics 7, 361-366.

614   J Murlis, J S Elkinton, a., Cardé, R.T., 1992. Odor Plumes and How Insects Use Them. Annual
615   Review of Entomology 37, 505-532.

616   Jones, P.L., Agrawal, A.A., 2017. Learning in Insect Pollinators and Herbivores. Annual Review of
617   Entomology 62, 53-71.

618   Jordan, A., Haidacher, S., Hanel, G., Hartungen, E., Mark, L., Seehauser, H., Schottkowsky, R.,
619   Sulzer, P., Mark, T.D., 2009. A high resolution and high sensitivity proton-transfer-reaction time-
620   of-flight mass spectrometer (PTR-TOF-MS). International Journal of Mass Spectrometry 286,
621   122-128.

622   Knudsen, J.T., Eriksson, R., Gershenzon, J., Ståhl, B., 2006. Diversity and distribution of floral
623   scent. The Botanical Review 72, 1.

624   Krol, M.C., Molemaker, M.J., de Arellano, J.V.G., 2000. Effects of turbulence and heterogeneous
625   emissions on photochemically active species in the convective boundary layer. Journal of
626   Geophysical Research: Atmospheres 105, 6871-6884.

627   Mafra-Neto, A., Cardé, R.T., 1994. Fine-scale structure of pheromone plumes modulates upwind
628   orientation of flying moths. Nature 369, 142-144.

629   Matsumoto, Y., Menzel, R., Sandoz, J.-C., Giurfa, M., 2012. Revisiting olfactory classical
630   conditioning of the proboscis extension response in honey bees: A step toward standardized
631   procedures. Journal of Neuroscience Methods 211, 159-167.

632   Nazaroff, W.W., Weschler, C.J., 2022. Indoor ozone: Concentrations and influencing factors.
633   Indoor Air 32, e12942.

634   Reitmayer, C.M., Girling, R.D., Jackson, C.W., Newman, T.A., 2022. Repeated short-term
635   exposure to diesel exhaust reduces honey bee colony fitness. Environmental Pollution 300,
636   118934.

637   Riffell, J.A., Shlizerman, E., Sanders, E., Abrell, L., Medina, B., Hinterwirth, A.J., Kutz, J.N., 2014.
638   Flower discrimination by pollinators in a dynamic chemical environment. Science 344, 1515-1518.

639   Ryalls, J.M.W., Langford, B., Mullinger, N.J., Bromfield, L.M., Nemitz, E., Pfrang, C., Girling, R.D.,
640   2022. Anthropogenic air pollutants reduce insect-mediated pollination services. Environmental
641   Pollution 297, 118847.

642   Saunier, A., Grof-Tisza, P., Blande, J.D., 2023. Effect of ozone exposure on the foraging
643   behaviour of Bombus terrestris. Environmental Pollution 316, 120573.

644   Szyszka, P., Gerkin, R.C., Galizia, C.G., Smith, B.H., 2014. High-speed odor transduction and
645   pulse tracking by insect olfactory receptor neurons. Proceedings of the National Academy of
646   Sciences 111, 16925-16930.

647   Vanderplanck, M., Lapeyre, B., Brondani, M., Opsommer, M., Dufay, M., Hossaert-McKey, M.,
648   Proffit, M., 2021. Ozone Pollution Alters Olfaction and Behavior of Pollinators. Antioxidants 10,
649   636.

650 Vingarzan, R., 2004. A review of surface ozone background levels and trends. Atmospheric
651 Environment 38, 3431-3442.

652 Williams, J., Ringsdorf, A., 2020. Human odour thresholds are tuned to atmospheric chemical
653 lifetimes. Philosophical Transactions of the Royal Society B: Biological Sciences 375, 20190274.

654 Zhang, J., Wei, Y., Fang, Z., 2019. Ozone Pollution: A Major Health Hazard Worldwide. Frontiers
655 in Immunology 10.

656

657

658

659

660

661

662

663

664

665

666

667

668

669

670

671

672

673

674

675

676

677

678

679
680

Highlights:

- Ozone pollution degrades the components of floral odour plumes
- Reaction rates were fastest at the plume edges and slowest at the plume centre
- Higher O_3 levels increased plume intermittency and reduced odour filament width
- Bees recognition of floral odours declined significantly following reaction with O_3

Declaration of interests

☒ The authors declare that they have no known competing financial interests or personal relationships that could have appeared to influence the work reported in this paper.

☐The authors declare the following financial interests/personal relationships which may be considered as potential competing interests: